Biophysical Journal, Volume *117*

Supplemental Information

Particle-Based Simulation Reveals Macromolecular Crowding Effects on the Michaelis-Menten Mechanism

Daniel R. Weilandt and Vassily Hatzimanikatis

Supporting Material for:

Particle-based simulation reveals macromolecular crowding effects on the Michaelis-Menten mechanism

Daniel R. Weilandt, Vassily Hatzimanikatis

Measuring the bimolecular elementary rates

As described in the main text, the effective bimolecular rate constant can be extracted from the effective collision frequency $z_{A,B}$ between two species, A and B. This collision frequency is estimated as the number of collisions between A and B in an integrated time interval $c_{A,B}(t, t + \Delta t)$ per time step Δt:

$$z_{A,B}(t, t + \Delta t) = \frac{c_{A,B}(t,t+\Delta t)}{\Delta t}. \qquad \text{(S1)}$$

In Supporting Figure (1) two examples for time traces of collisions per time interval for a reaction limited association of S and E are presented. From the running mean, it can be seen that the there is no obvious time dependency of the collision frequency observable. This results is enforced by the fact the distribution of the collisions at the beginning, the end and over the complete measurement intervall follow a similar distribution.

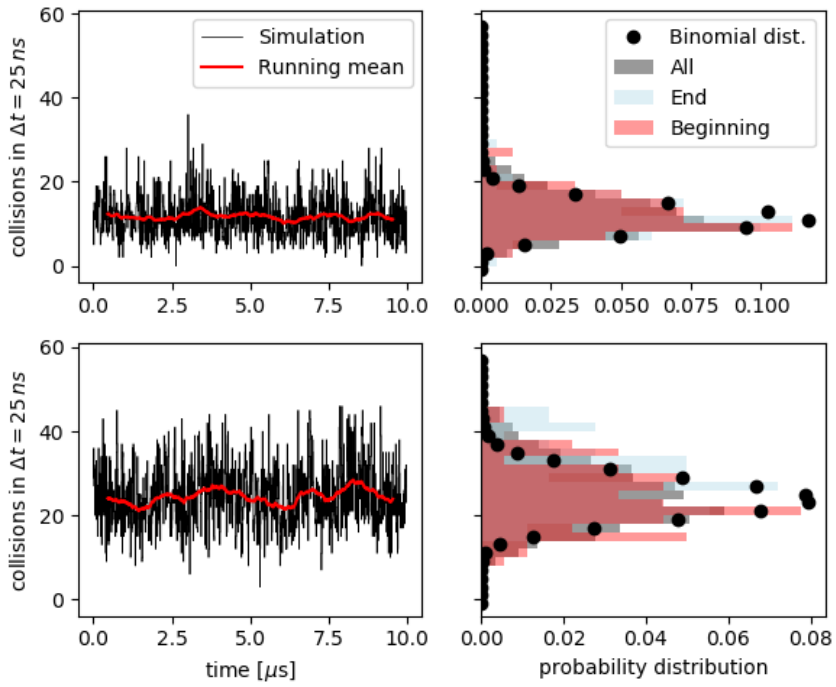

Supporting Figure 1: Left column time traces of collision events between E and S as a function of time and the running mean over 100 time intervals. Right column histograms of all data point of the collisions time trace (All), the first (Beginning) and the last (End) 100 data points compared with a binomial distribution where $p = \langle c_{E,S} \rangle / N_E N_S$ and $n = N_E N_S$. The upper row show the results with $\phi = 0\,\%$ the lower row for $\phi = 40\,\%$ for the *E. Coli* as described in the main text.

Regression for GEEK parameters

When investigating the measured relative rate constants for pgm as a function of the individual rate constants it can be seen that there is no dependency of the rate constants with respect to the individual concentration. Only an increase in the conditional variance towards smaller concentrations can be seen, see Supporting Figure (3). Thus ordinary least squares (OLS) fitting cannot be applied as the data exhibits heteroscedasticity. We show that we obtain normally distributed residuals by weighting the data points by the inverse of the conditional standard deviation $\sqrt{V(R|X)}$, where X is the n-dimensional input variable of the regression model and R are the residuals of the OLS output variable. In Supporting Figure (2) it can be clearly seen that the weighted residuals resemble a normal distribution.

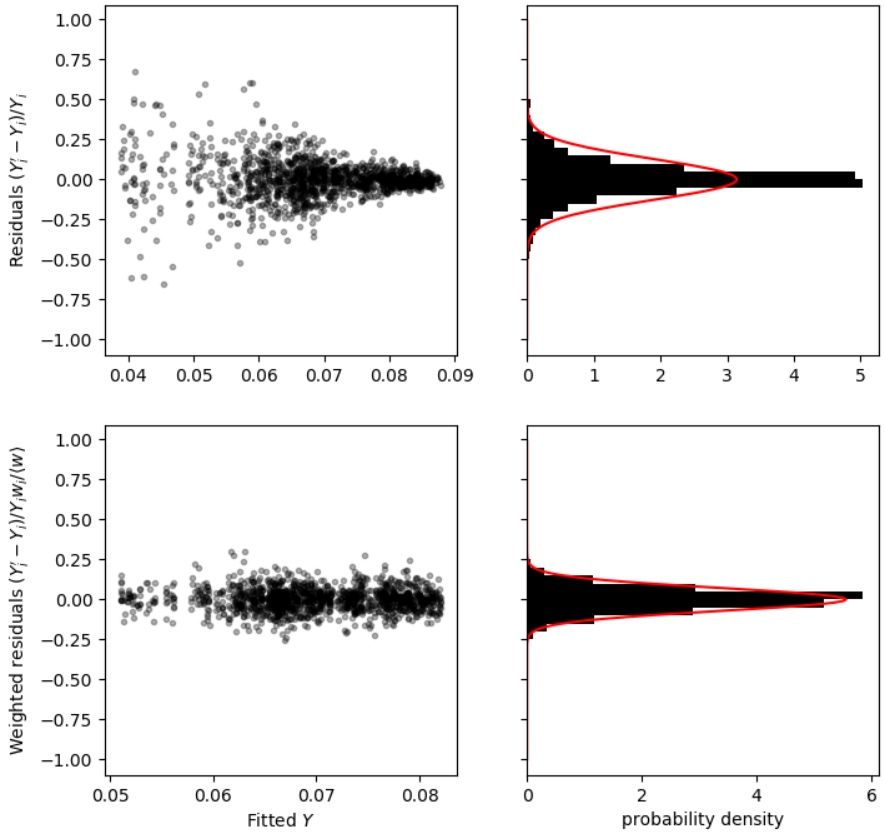

Supporting Figure 2: Model results for OLS and WLS for the model output $Y_i = \log(k_{1,f,eff,i} / k_{1,f,0})$. Left column: Residuals vs. fitted output values Y_i'. Right column: Probability density of the residuals. Upper row: Residuals of the OLS model. Lower row: Effective residuals of the WLS model

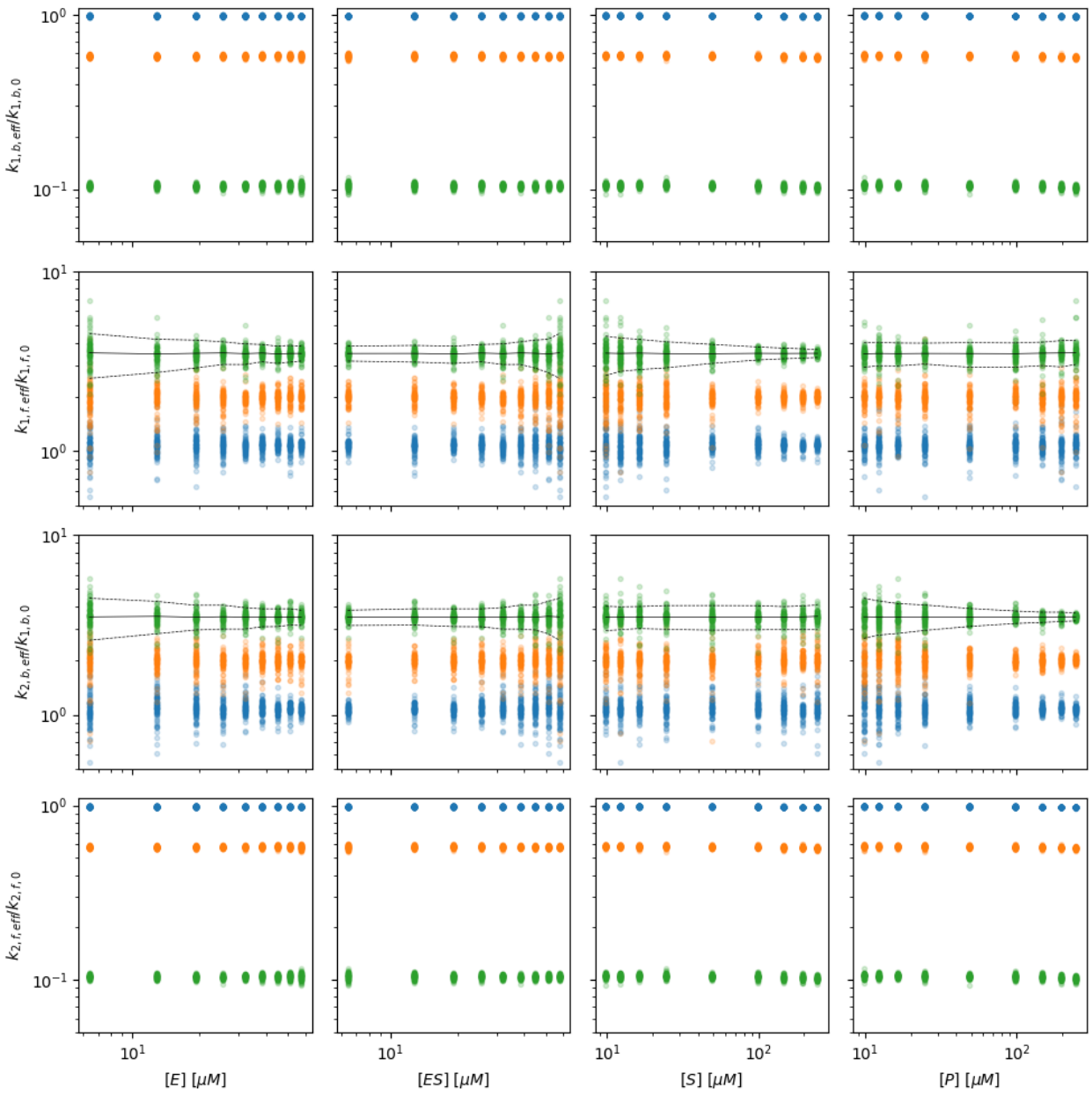

Supporting Figure 3: Projection of the simulated data points onto the respective concentration axis for (blue) $\phi = 0\%$ (orange) $\phi = 30\%$ and (green) $\phi = 50\%$ inert volume fraction with the *E. Coli* size distribution. The black line denoted the conditional mean and the dashed line denoted the conditional 5% and 95% percentiles at the corresponding concentration value for $\phi = 50\%$ inert volume fraction.

Validation of GEEK

In the following section, we first validated whether the results of the GEEK approximation are in agreement with detailed openbread simulations as described in the main text. Second, we validated whether geek is also able to capture the results of the crowder free Cichocki-Hinsen algorithm (1). To perform these comparisons, we used a simple association-dissociation model with two different parameter sets:

$$A + B \underset{k_f K_D}{\overset{k_f}{\rightleftharpoons}} C \tag{S2}$$

Computational details of the validation simulations

The two parameter sets only differ in their association rate the remaining model parameters considered a diffusion coefficient $D_{A/B} = 500\ \mu\mathrm{m}^2\mathrm{s}^{-1}$ a mass $m_{A/B} = 10\ \mathrm{kDa}$ and collision radius $r_{A/B} = 2\ \mathrm{nm}$ for the species A and B, a diffusion coefficient $D_C = 350\ \mu\mathrm{m}^2\mathrm{s}^{-1}$, a mass $m_C = 20\ \mathrm{kDa}$ and collision radius $r_C = 3\ \mathrm{nm}$ for the species C and a cubic simulation volume $V = 10^{-18}\ \mathrm{L}$. For the reaction parameters we consider a dissociation constant $K_D = 50\ \mu\mathrm{M}$ and an association rate constant $k_{f,diff} = 5 \times 10^9 \mathrm{M}^{-1}\mathrm{s}^{-1}$ ($k_{f,diff}/\gamma_{A,B} \approx 5$) for the diffusion controlled case. Whereas for the reaction controlled case we consider an association rate constant $k_{f,react} = 5 \times 10^7 \mathrm{M}^{-1}\mathrm{s}^{-1}$ ($k_{f,react}/\gamma_{A,B} \approx 500$). To simulate crowding we introduced inert molecules of the size $2.6\ \mathrm{nm}$ at different volume fractions. As in the case presented in the main text, the dynamics viscosity of the liquid between the particles was assumed to be water with $0.7\ \mathrm{Pa\,s}$ at the $T = 310.15\ \mathrm{K}$. The system is considered to be isothermal $T = \mathrm{const}$. To compare the methods we simulate ten independent time traces for an initial rate experiment with the initial concentrations $[A] = [B] = 50\ \mu\mathrm{M}$ and $[C] = 0\ \mu\mathrm{M}$.

To apply the GEEK framework each timestep all possible first-order reactions are attempted $L = 100$ times. For the regression input space, all combinations of substrate and product concentrations that were n_i-fold increased and n_d-fold decreased with respect to the reference concentrations $[A]_0 = [B]_0 = [C]_0 = 50\ \mu\mathrm{M}$ were used, with $n_i \in [1,2]$ and $n_u \in [1,2,4]$. Each sampled concertation state is simulated $1\ \mu\mathrm{s}$ where the first $0.5\ \mu\mathrm{s}$ are discarded Furthermore, ten independent realizations of the crowding population were used for every concentration sample to capture the variability that comes from differently sized crowding-agents drawn from the size distribution.

Validation of GEEK based on hard sphere Brownian reaction dynamics

In a first step we compare the time traces for GEEK and openbread for the dilute case, i.e. without any inert molecules, see Supporting Figure 5 left column. The results show that for the reaction controlled case GEEK is able to capture the mean dynamics of the detailed openbread very well, for the diffusion controlled case the mean dynamics of the initial rate is captured very well but a slight deviation of the equilibrium concentration $[A]$ is visibel.

In a next step we characterized the distribution of [A] close to equilibrium, i.e $t \geq 500\ \mu s$ in the reaction controlled and $t \geq 5\ \mu s$ in the diffsion controlled case, for different inert volume fraction ϕ, see Supporting Figure 5 right column. It can be seen that for higher volume fractions of inert modelcules both the GEEK and the openbread resuts show that the equilirbium is shifted towards the production of $[C]$, i.e. the equlibrium concentration $[A]$ drops with increasing volume fraction. We also observe that for higher volume fractions the difference between the mean of $[A]$ in openbread and GEEK is reduced.

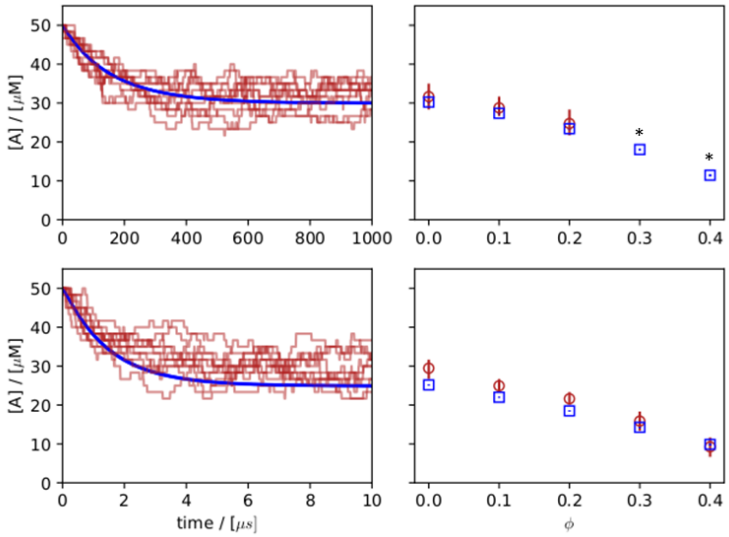

Supporting Figure 4: Concentration of $[A]$ as a function of time t for $\phi = 0$ for GEEK (blue) and openbread (red) (left column) and concentration in equilibrium for different ϕ (right column). For the reaction controlled case (upper row) and the diffusion controlled case (lower row). *A hard sphere Brownian reaction dynamics simulation of these data points was not feasible within the time frame of this review.

Finally, we compared the initial reaction rate characterized as the mean change of the reactant [A] over an initial time interval $[0, t_{init}]$, where $t_{init} = 0.5$ µs for the diffusion limited case and $t_{init} = 50$ µs for the reaction limited case (see Supporting Figure 5). Similar to the equilibrium properties we see that the GEEK model is able to capture the mean initial rate of the hard-sphere Brownian reaction dynamics

model. It also can be seen that in the reaction limited case the GEEK approximation is in close agreement to the detailed simulation. In both cases does geek capture the increase of the initial rate visible in the hard-sphere Brownian reaction dynamics.

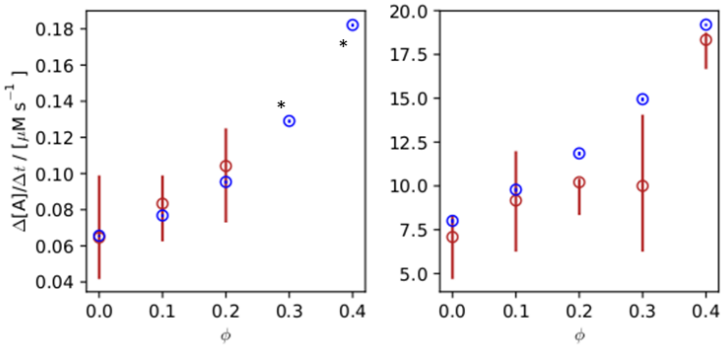

Supporting Figure 5: Initial reaction rate measured as the mean change of $[A]$ for GEEK (blue) and openbread (red) measured for different ϕ, for the reaction controlled case (left) and the diffusion controlled case (right). *A hard sphere Brownian reaction dynamics simulation of these data points was not feasible within the time frame of this review.

Validation of GEEK based on the crowder free Cichocki-Hinsen algorithm

To provide further evidence that GEEK is able to approximate the behavior of high-cost simulations based on the first physical principle we simulate the association-dissociation system described above using the crowder free Cichoki-Hinsen algorithm (1). As described above we compare the concentrations for $t \geq 500\ \mu s$ in the reaction controlled and $t \geq 5\ \mu s$ in the diffsion controlled case as well as the initial reaction for $t \leq 0.5$ µs in the diffusion limited case and $t \leq 50$ µs in the reaction limited case. We again show that the GEEK models are able to approximate the dynamics of the high cost model. More importantly, GEEK models are able to approximate the effects crowding has on the initial rate experiment. For both cases, GEEK is able to capture the trends of approximation for the equilibrium concentrations (see Supporting Figure 6) and the initial reaction rates (see Supporting Figure 7). When comparing the initial reaction rates we observe that the estimated reaction limited initial reactions rates are in better agreement with the GEEK approximation then the corresponding diffusion limited initial reaction rates (see Supporting Figure 7).

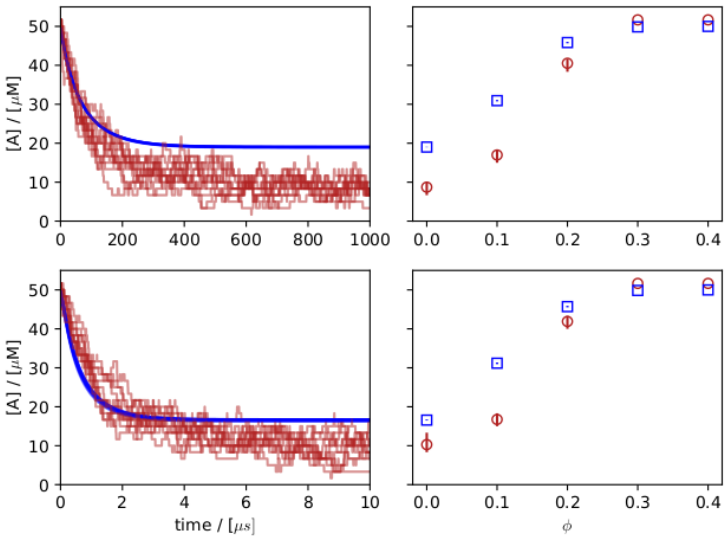

Supporting Figure 6: Concentration of $[A]$ as function of time t for $\phi = 0$ for GEEK-CFCH (blue) and CFCH (red) (left column) and concentration in equilibrium for different ϕ (right column). For the reaction controlled case (upper row) and the diffusion controlled case (lower row).

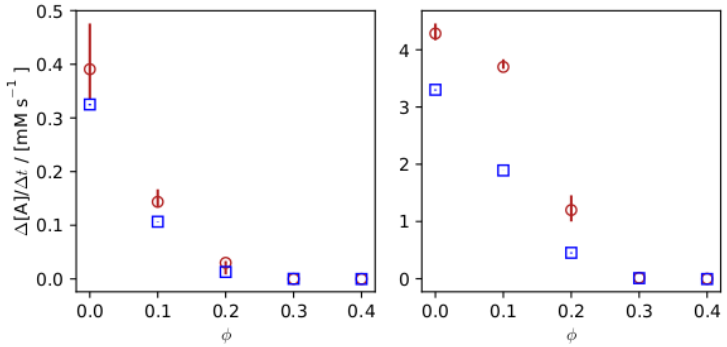

Supporting Figure 7: Initial reaction rate measured as the mean change of $[A]$ for GEEK- CFCH (blue) and CFCH (red) measured for different ϕ, for the reaction controlled case (left) and the diffusion controlled case (right).

Discussion on the results of the HSBRD and CFCH simulations

A comparison between figures S4 and S6 as well as S5 and S7 show that the hard-sphere Brownian dynamics algorithm and the crowder free Cichoki-Hinsen algorithm are not yielding the same results for the same crowding conditions. We suspect that the difference in the crowding sensitivity originates from the difference in the collision model of the two algorithms. The hard-sphere Brownian dynamics algorithm models every non-reactive collision as an explicit elastic hard sphere collision (see Supporting Figure 8 b)) both the Cichoki-Hinsen algorithm and the crowder-free Cichoki-Hinsen algorithm are

rejecting the propagation moves that would lead to overlap. In this work, we used the hard-sphere Brownian dynamics algorithm as described by Strating as it was successfully applied his algorithm to non-equilibrium systems of hard-spheres (2). The algorithm presented by Cichoki and Hinsen (3) is only valid to obtain the correct radial distribution functions in equilibrium systems. They show that for non-equilibrium systems an additional non-overlap correction has to be implemented (3). This correction is not implemented in the crowder-free Cichoki-Hinsen algorithm (1). Therefore, we acknowledge that the model predictions for these simulations strongly depend on the microscopic model. Nevertheless, we showed that independent of the microscopic simulation method GEEK models are able to approximate the dynamic behavior of the complex particle simulation. Thus GEEK can be used as a reliable method to capture the dynamics of crowed enzyme kinetics and incorporate crowded behavior into larger scale kinetic models.

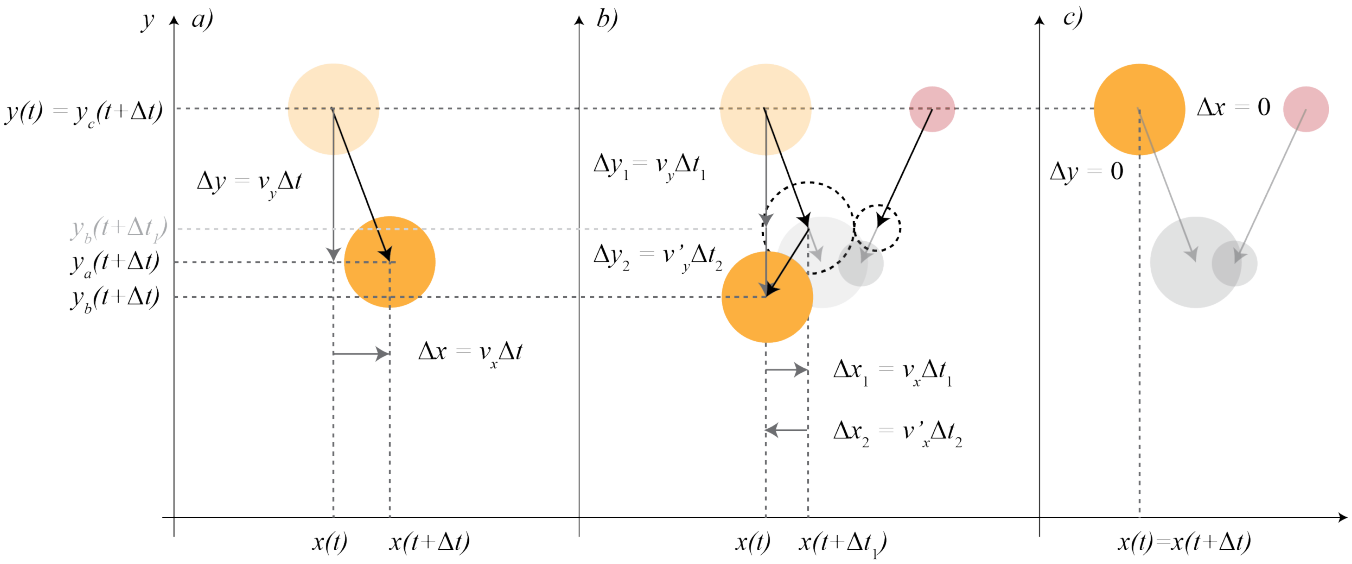

Supporting Figure 8: Comparison of different propagation schemes. a) Brownian motion where the propagation is simply determined by the velocity v drawn from the respective velocity distribution function. b) Explicit elastic hard sphere collision, particles are moved with the initial velocity v until time $t + \Delta t_1$ when the collision occurs. The velocities are updated according to the law of momentum conservation then propagated for remaining part of the time step $\Delta t_2 = \Delta t - \Delta t_1$. c) Propagation according to the Cichoki-Hinsen algorithm where the collision is simply rejected if the hypothetical positions after the time Δt lead to an overlap with another particle.

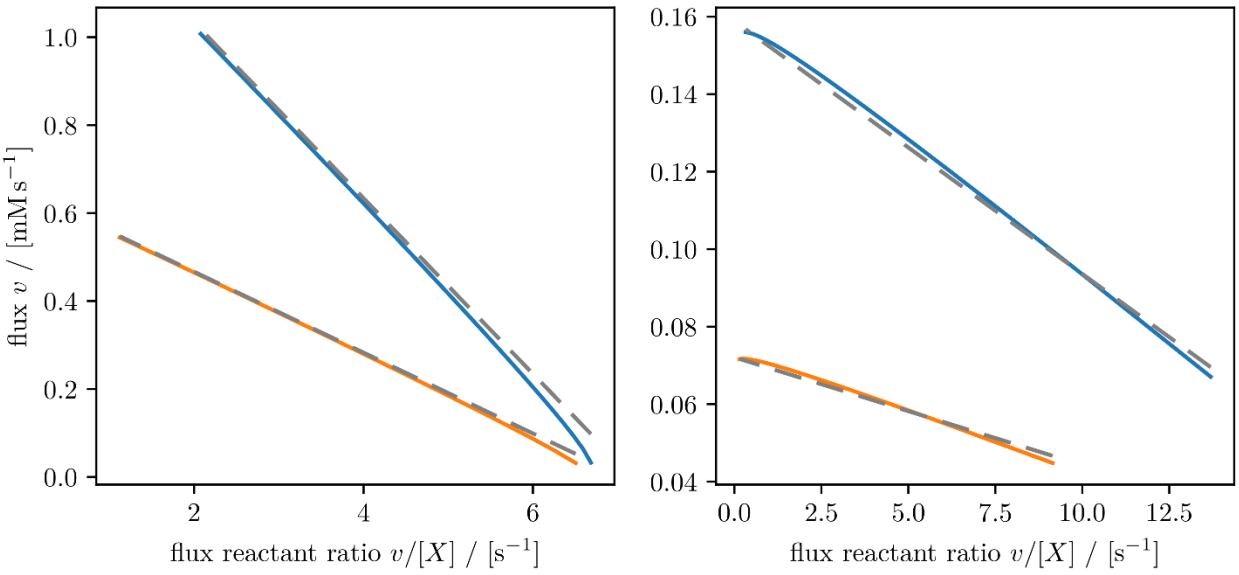

Supporting Figure 9: Eadie–Hofstee diagrams of the quasi-steady state flux v for inert volume fractions of (left) $\phi = 0\,\%$ and (right) $\phi = 50\,\%$. The dotted lines represent the respective result of a linear regression.

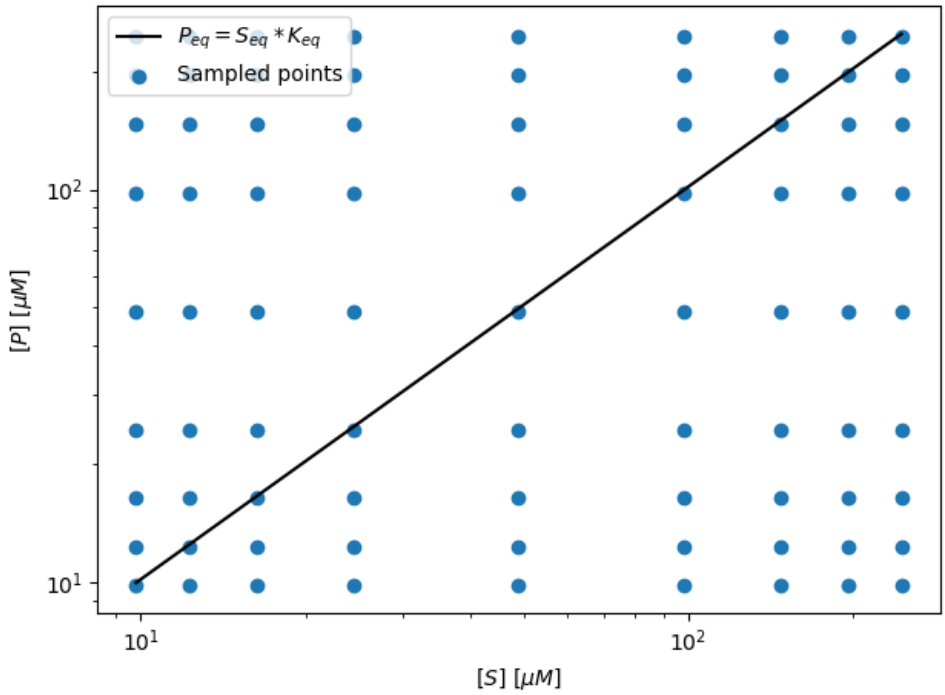

Supporting Figure 10: Sampled state space of $[S]$ and $[P]$ compared to the equilibrium concentrations $K_{eq} = P_{eq}/S_{eq}$.

Supporting References

1. Smith, S., and R. Grima. 2017. Fast simulation of Brownian dynamics in a crowded environment. Journal of Chemical Physics 146(2).
2. Strating, P. 1999. Brownian dynamics simulation of a hard-sphere suspension. Phys Rev E 59(2):2175-2187.
3. Cichocki, B., and K. Hinsen. 1990. Dynamic Computer-Simulation of Concentrated Hard-Sphere Suspensions .1. Simulation Technique and Mean-Square Displacement Data. Physica A 166(3):473-491.